ISSN 1027-5495. Functional Materials, 30, No.2 (2023), p. 156-162.
doi:https://doi.org/10.15407/fm30.02.156

Morphological investigations of solid solutions $(GaAs)_{1-x}(ZnSe)_x$ doped with <Sb>

A.Sh.Razzokov

Urgench State University, 14 Kh. Alimdjan, Urgench, Uzbekistan

Received March 5, 2023

The possibility of growing $(GaAs)_{1-x}(ZnSe)_x$ solid solutions doped with antimony at the onset of crystallization at a temperature T_{OC} = 750°C on a GaAs(100) and GaAs(111) substrates is shown. The method of liquid-phase epitaxy from a limited solution-melt of tin in the cooling rate range of 0.5–3 deg/min was used. The chemical composition, the perfection of the substrate-film boundary, and the surface of the epitaxial layers of $(GaAs)_{1-x}(ZnSe)_x$ <Sb> solid solutions were studied using a scanning electron microscope (SEM); the surface roughness of the films was studied using an atomic force microscope (AFM). It is shown that doping of the solid solution with Sb reduces the dislocation density on the film surface to $N_d = 7\cdot10^3$ cm^{-2}, and on the substrate-film interface — to $N_d = 2\cdot10^4$ cm^{-2}. X-ray diffraction studies have shown that the resulting films are single-crystal and have a sphalerite structure. Some electrophysical and photoelectric properties of the samples have been studied.

Keywords: solid solution, dislocation, epitaxy, impurity, heterostructure.

Морфологічні дослідження твердих розчинів $(GaAs)_{1-x}(ZnSe)_x$, легованих <Sb>. *А.Ш.Раззоков*

Показана можливість вирощування твердих розчинів $(GaAs)_{1-x}(ZnSe)_x$ легованих сурмою на підкладках GaAs(100) та GaAs(111) при температурі кристалізації T_{OC} = 7500°C методом рідкої фази. Показана епітаксія з обмеженого розчину-розплаву олова в діапазоні швидкостей охолодження 0,5–3 град./хв. Хімічний склад, досконалість межі підкладка — плівка та поверхню епітаксійних шарів твердих розчинів $(GaAs)_{1-x}(ZnSe)_x$ <Sb> досліджували за допомогою скануючого електронного мікроскопа (РЕМ) а шорсткість поверхні плівок досліджували за допомогою атомно-силового мікроскопа (АСМ). Показано, що легування твердого розчину сурмою Sb зменшує щільність дислокацій (на поверхні плівки $N_d = 7\cdot10^3$ cm^{-2}, на гетерограниці підкладка-плівка $N_d = 2\cdot10^4$ cm^{-2}). Рентгеноструктурні дослідження показали, що отримані плівки є монокристалічними і мають структуру сфалериту. Досліджено деякі електрофізичні та фотоелектричні властивості зразків.

1. Introduction

At present, on the basis of chemical compounds of types $A^{III}B^{V}$, $A^{II}B^{VI}$, obtaining direct-gap semiconductor solid solutions with a controlled composition, having specific electrophysical and photoelectric properties, is an urgent task for creating new materials and structures for instrumentation.

Of particular interest is the heterojunction formed between GaAs and ZnSe semiconductor compounds, which have interesting photoelectric properties and similar lattice parameters (discrepancy of ~ 0.25 %), which makes it possible to obtain a heterojunction without a significant number of defects, dislocations at the interface. Solid solutions based on the GaAs–ZnSe system make it possible to vary the main electrical parameters of a semiconductor material over a wide range with a change in their chemical composition. It is possible to choose materials with optimal characteristics when creating specific semiconductor devices.

The growth of $(GaAs)_{1-x}(ZnSe)_x$ epitaxial layers on GaAs substrates provides a reduction to a minimum of stresses arising due to the mismatch between the crystal lattices of the substrates and films. The emerging dislocations at the substrate-film interface and along the film growth direction can be additional recombination centers, which worsens the injection properties in heterojunctions. They also significantly reduce the separation factor of electron-hole pairs generated by light in photoelectric converters. Therefore, it still remains a problem to obtain a high value of efficiency in photocells.

In [1, 2], we have shown how to obtain $(GaAs)_{1-x}(ZnSe)_x$ solid solutions from a tin and lead solution-melt on a GaAs substrate by program forced cooling. There the structural perfection of the grown epitaxial layers, structures, including its morphology, was studied. The optimal technological growth regime for obtaining crystalline perfect $(GaAs)_{1-x}(ZnSe)_x$ films and GaAs–$(GaAs)_{1-x}(ZnSe)_x$ structures has been established.

It has been sufficiently studied by many authors how to obtain GaAs–ZnSe, ZnSe–GaAs heterostructures with the smallest defects and the best crystal perfection with different growing methods. But there are significant unsolved problems in this field.

In [3], the effect of the initial growth regime on the structure of dislocations in ZnSe epitaxial layers grown on GaAs(100) by molecular beam epitaxy is presented. The process of crystal growth and the distribution of dislocations in the ZnSe/GaAs(100) system have been studied. When the initial growth occurred through the formation and coalescence of three-dimensional islands, the density of threading dislocations turned out to be an order of magnitude higher, and the misfit dislocation lengths were significantly smaller than in the case of the initial growth in the two-dimensional layer-by-layer regime.

It was reported in [4] that the addition of isoelectronic impurities (Sb doping) into GaAs reduces the dislocation density in this crystal. The model described in this article explains the major importance of isoelectronic doping for controlling the stoichiometry of a solid, including the production of zero dislocation density GaAs and semi-insulating GaAs. Several effects have been proposed to explain these phenomena, the most common of which claims that a still unknown mechanism affects the stoichiometry of a solid.

To obtain a high-resistance GaAs single crystal, it was doped with Sb. Hall and photoluminescence measurements of a series of samples showed a new donor level located 0.48 eV below the edge of the conduction band. This level reduced the resistivity of the material. A comparison was made with known eigenlevels in the undoped material and the 0.48 eV donor was shown to be different from either of them. It was concluded that the defect with a donor level of 0.48 eV is associated with an impurity SbGa antisite isolated or in complex with intrinsic defects [5].

It was shown in [6] that isoelectronic doping with antimony reduces the number of traps and improves material properties during the epitaxial growth of doped GaAs(100). The influence of the antimony dopant on the optimal growth temperature was studied in order to obtain high-quality heterostructures at lower temperatures. High-quality GaAs films were grown by molecular beam epitaxy at growth temperatures of 610°C and 50°C below this temperature using Sb as a dopant. The electrical properties of the films were then investigated using Hall mobility measurements and spectroscopy. Doping GaAs with antimony makes it possible to reduce the density of traps.

GaAs epitaxial layers doped with Sb are grown by liquid-phase epitaxy (LPE). Hall measurements show that doping increases the mobility of charge carriers and a sharp drop in the density of the traps [7].

The paper [8] describes the production of $GaAs_{1-x}Sb_x$ nanowires by molecular beam epitaxy on a GaAs substrate. The grown $GaAs_{1-x}Sb_x$ nanowires have the crystal structure of pure zinc blende. Rectifying transistors based on individual $GaAs_{1-x}Sb_x$ nanowires were fabricated.

Obtaining *p*-type zinc selenide is a difficult task in the crystal growth technology. Therefore, for the growth of the acceptor type ZnSe, Sb was used as a dopant [9, 10].

The authors of [11] also characterized the atomic structure of extended defects in $GaAs/GaAs_{1-x}Sb_x/GaAs(001)$ heterostructures using transmission electron microscopy. The defects located at the $GaAs/GaAs_{0.34}Sb_{0.66}$ interface under tension do not have an edge component in the projection plane and is identified either as dissociated screw dislocations or as partial dislocation dipoles, i.e. dislocation densities decrease.

The effect of doping with Sb on the structural and optical properties of $Zn_{1-x}Sb_xSe$ thin films obtained by thermal evaporation on a glass substrate has been studied. Various characterization methods such as X-ray diffraction (XRD), energy-dispersion spectrometry (EDS), Raman spectroscopy, and spectroscopic ellipsometry were used to evaluate the structural and optical properties of the deposited films. X-ray phase analysis showed the formation of a polycrystalline cubic structure, with orientation (111) without any signs of secondary phases. The crystallographic parameters indicated a structural modification in the ZnSe films with Sb inclusions. The results of spectroscopic ellipsometry showed a decrease in the band gap of the film (from 2.61 eV to 1.81 eV) with increasing Sb content [12].

The paper [13] shows the possibility of obtaining crystalline $Si_{1-x-y}Ge_xSn_y$ epitaxial layers and $Si–Si_{1-x}Ge_x–Si_{1-x-y}Ge_xSn_y$ structures using the liquid epitaxy method. The high perfection of the functional structures was ensured by smoothing the difference in the lattice parameters between the substrate and a film (due to a smooth change in the chemical composition of the film) along its growth direction. The dislocation density at the substrate-film boundary was $N_D \sim 10^5$ cm^{-2}, and on the film surface, $N_D \sim 9\cdot10^3$ cm^{-2}.

It is shown that $Si_{1-x-y}Ge_xSn_y$ films and $Si–Si_{1-x}Ge_x–Si_{1-x-y}Ge_xSn_y$ structures with the lowest dislocation densities can be obtained by the method of liquid-phase epitaxy, relative to other discrete heterostructures.

This article is devoted to the technological features of obtaining heterostructures based on $(GaAs)_{1-x}(ZnSe)_x$ solid solutions, doping of which with Sb make it possible to reduce defects in epitaxial layers and film-substrate heterointerfaces. In addition, the Sb dopant creates a deep level inside the band gap and compensates for the majority charge carriers. Doping $(GaAs)_{1-x}(ZnSe)_x$ solid solution with Sb improves its crystalline perfection and electrophysical, photoelectric properties in comparison with the undoped film. Thus, the charge carrier concentration (n_p) decreases (from $\sim 2\cdot10^{18}\div10^{19}$ cm^{-3} to $\sim 3\cdot10^{16}\div10^{17}$ cm^{-3}), while the mobility (μ_p) increases ($30\div60$ cm^2/V·s to $70\div100$ cm^2/V·s). Taking into account the above, solid solutions $(GaAs)_{1-x}(ZnSe)_x$ doped with Sb can be used in the field of optoelectronic instrumentation as a semiconductor material.

2. Experimental

This paper presents the results of experimental studies of epitaxial layers of $(GaAs)_{1-x}(ZnSe)_x$ solid solution obtained from a limited solution-melt (Sn–Sb–GaAs–ZnSe) on a GaAs substrate. At the crystallization onset temperature T_{OC} = 750°C, epitaxial layers $(GaAs)_{1-x}(ZnSe)_x$ doped with Sb were grown with forced cooling of 1 deg/min. The substrates had a crystallographic orientations (100) and (111), electrical resistivity $\rho > 10^7$ Ω·cm, *p*- and *n*-type conductivity ($p = 1.1\cdot10^{17}$ cm^{-3}, $n = 3\cdot10^{17}$ cm^{-3}), 20 mm in diameter and ~ 400 μm thick.

The quality of epitaxial layers is largely determined by the preparation of the substrate surface. Therefore, the GaAs substrates were subjected to chemical treatment using a polishing etchant of the following composition: $1hHNO_3 + 3hHCl + 2hH_2O$. The substrate was etched with active movement of the etchant for 5–7 minutes. Next, the substrates were washed by adding deionized water to the etchant until the acidic components of the solution were eliminated.

The growth of the epitaxial layer was carried out from the volume of a tin solution-melt bounded by two substrates in an atmosphere of hydrogen purified by palladium. A detailed description of the technique used is presented in [14].

To prepare a liquid solution-melt, the solubilities of GaAs and ZnSe in Sn were determined in the temperature range of 780–450°C by weight loss of gallium arsenide and zinc selenide samples placed in liquid tin and kept in it until the solution was saturated. In this case, the influence of GaAs on the solubility of ZnSe was taken into account. The composition of the Sn–GaAs–ZnSe melt solution was calculated on the basis of published data and the results of preliminary experiments, taking into account the solubility of binary components [15].

The content of the chemical composition and the perfection of the substrate-film boundary of epitaxial layers of $(GaAs)_{1-x}(ZnSe)_x$ solid solutions were studied using a Tescan Vega 3 LMH scanning electron microscope equipped with a Bruker XFlash 5010 X-ray energy dispersive detector.

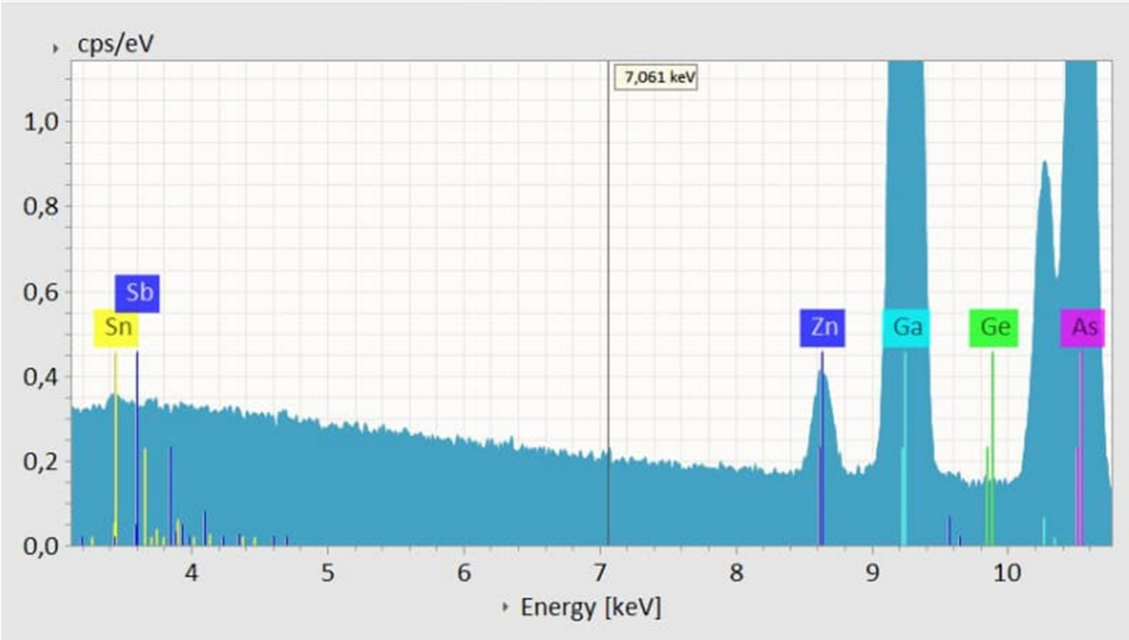

Fig. 1. EDS spectrum of the cleavage of GaAs–$(GaAs)_{1-x}(ZnSe)_x$ structures.

The crystallographic characteristics of the grown $(GaAs)_{1-x}(ZnSe)_x$ solid solutions were studied by high-resolution X-ray diffraction (GID and GONIO modes using HR-XRD, Panalytical/Empyrean). Prior to structural analysis, 2θ was calibrated with an error probability of ±0.02°. Standard line positions and line shapes for powder diffraction [silicon (Si) powder] were applied. The certified lattice parameter at 22.5°C was 0.5431179 nm±0.000008 nm. Since the sample is single-crystal, XRD studies used its rotation around the vertical axis.

The morphology and surface roughness of the films were characterized using an atomic force microscope (AFM) CoreAFM.

The epitaxial layers with the best parameters were obtained at a distance between the upper and lower substrates of 1–1.5 mm and in the cooling rate range of 0.5–2 deg/min. The grown $(GaAs)_{1-x}(ZnSe)_x$ films doped with Sb had a hole type of conductivity. Depending on the parameters of the technological process, the thickness of the grown films ranged from several to 25 μm.

3. Results and discussion

The content of the chemical composition and the perfection of the substrate-film boundary of epitaxial layers of $(GaAs)_{1-x}(ZnSe)_x$ <Sb> solid solutions were studied using a Tescan Vega 3 LMH scanning electron microscope equipped with a "Bruker XFlash 5010" characteristic X-ray detector. A general quantitative analysis of the composition from the end side (from the substrate to the film surface along the direction of growth in a step-by-step mode) of the GaAs–$(GaAs)_{1-x}(ZnSe)_x$ structures is performed. The EDS spectra obtained through cleavage are shown in Fig. 1.

The chemical elements of the components Ga, As, Zn, Se are the composition of the epitaxial layers of the $(GaAs)_{1-x}(ZnSe)_x$ solid solution, and antimony is present as an impurity (Table 1).

Figure 2 shows that the substrate-film boundary is smooth on all sides. This means that the growth of epitaxial layers from a saturated solution-melt of Sn–Sb–GaAs–ZnSe does not lead to subdissolution of the substrates, otherwise the structure of the substrate-film boundaries would be uneven.

The distribution of components over the end face of the epitaxial layers of the $(GaAs)_{1-x}(ZnSe)_x$ <Sb> sample (GaAs–$(GaAs)_x(ZnSe)_{1-x}$ structure) has been studied. The obtained results show almost uni-

Table 1. Quantitative content of chemical elements in $(GaAs)_{1-x}(ZnSe)_x$ solid solution

Elements	Atomic [%]
Ga	49.31
As	47.04
Zn	1.84
Se	1.81
Sum:	100

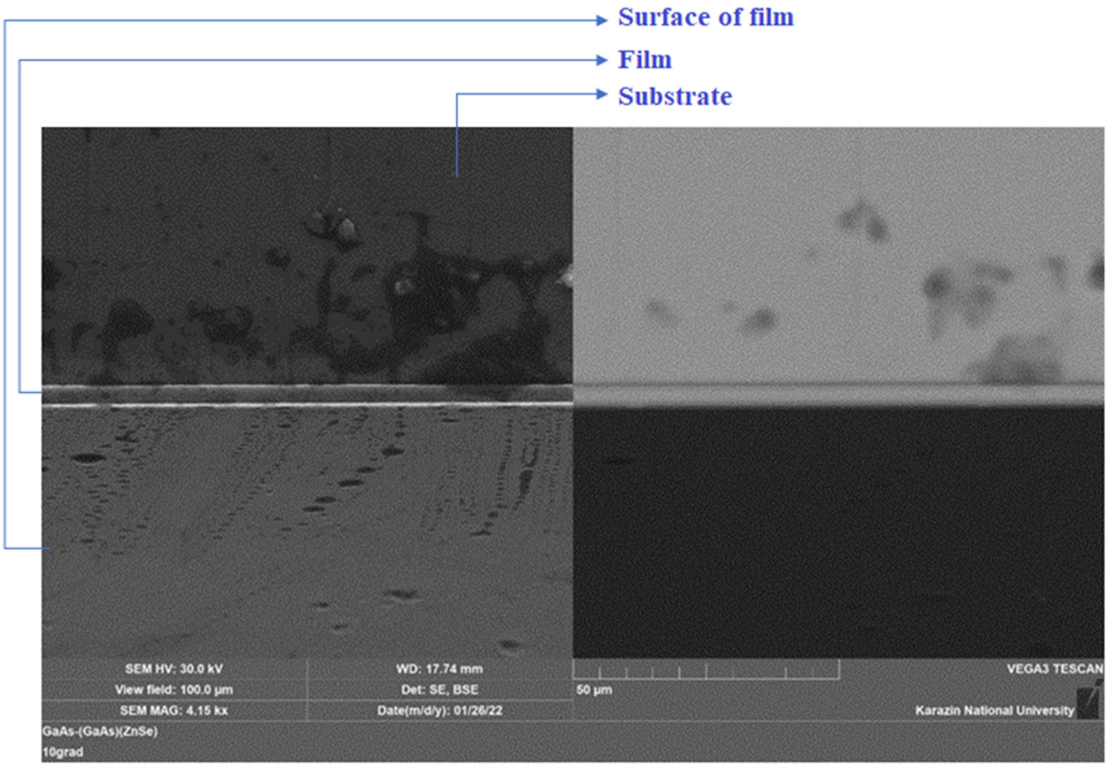

Fig. 2. A snapshot of a cleavage of GaAs–$(GaAs)_{1-x}(ZnSe)_x$ <Sb> structures obtained with a Tescan Vega 3 LMH scanning electron microscope.

formity ($0.96<x<0.97$) of the epitaxial layers of the $(GaAs)_{1-x}(ZnSe)_x$<Sb> solid solution along the growth direction and the film surface (Fig. 2).

The obtained epitaxial layers $(GaAs)_{1-x}(ZnSe)_x$ <Sb> were single-crystal and had the sphalerite structure. The X-ray diffraction pattern obtained from the sample $(GaAs)_{1-x}(ZnSe)_x$ <Sb> can be explained by the ordering of unit cells (Fig. 3).

The diffraction patterns show two doublets (400). The first one corresponds to the GaAs substrate according to the calculated lattice period a_{GaAs} = 5.6540±0.0001 Å. The second doublet obviously corresponds to the grown phase $(GaAs)_{1-x}(ZnSe)_x$ of the film. Moreover, the second doublet is shifted to larger Bragg angles, which indicated a decrease in the lattice period of the grown phase ($a_{(GaAs)1-x(ZnSe)x}$ = 5.6512±0.0001 Å). Since the lattice period of the ZnSe phase is larger (a_{ZnSe} = 5.6687±0.0001 Å) than that of the GaAs phase, the reason for the decrease in the lattice period of the grown phase may be tensile stresses arising on the surface (in the surface plane), tending to reduce the layer thickness, and therefore causing a decrease in the lattice period of the grown phase.

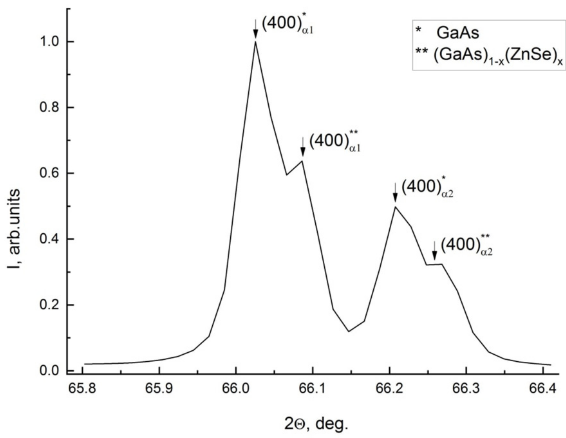

Fig. 3. Diffraction pattern obtained from a GaAs–$(GaAs)_{1-x}(ZnSe)_x$ sample/structures.

Depending on the technological conditions for the growth of a solid solution, it is possible to obtain structures GaAs–$(GaAs)_{1-x}(ZnSe)_x$, which determines the electrical and photoelectric properties of the grown films. The presence of dislocations causes a change in the microstructure, which is observed on the SEM image. However, doping of

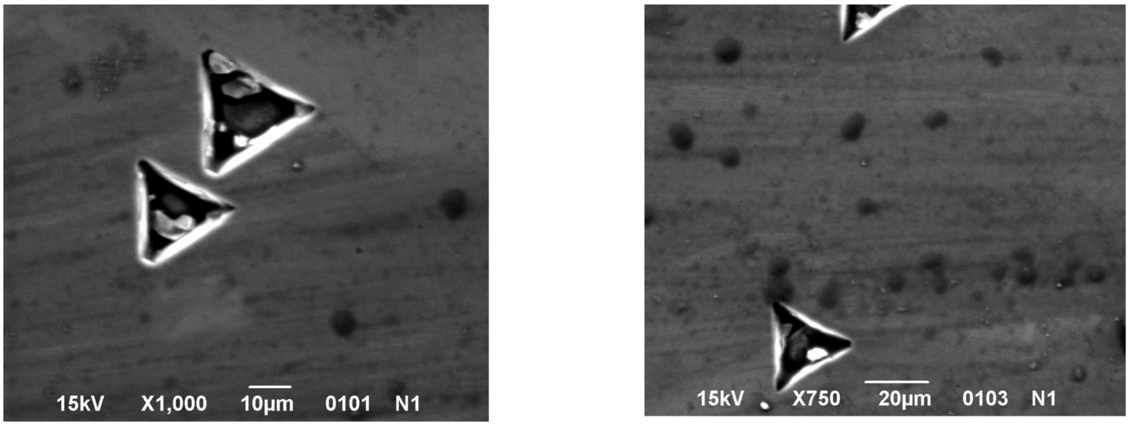

a **b**

Fig. 4. Dislocations of grown epitaxial layers $(GaAs)_{1-x}(ZnSe)_x$ doped with <Sb>: a) on the surface ($7\cdot10^3$ cm^{-2}); b) on the substrate-film heterointerface ($2\cdot10^4$ cm^{-2} scanning electron microscope EVO MA 10 (Zeiss)).

$(GaAs)_{1-x}(ZnSe)_x$ epitaxial layers with Sb significantly affects the crystalline perfection of the film; the dislocation density decreases both on the film surface and on the substrate-film heterointerface (Fig. 4).

To study the morphology of the obtained films, we selected the composition of the etchant consisting of mixtures of concentrated hydrofluoric (HF), nitric (HNO_3) and deionized water (H_2O) acids, in the ratios 1hHF + 2hHNO_3 + 4hH_2O. To reveal dislocation etch pits on the (111) plane, the samples were etched in the solution, then deionized water was diluted into the etchant and washed.

From Fig. 4 it can be seen that the dislocations are triangular in shape and oriented in the same direction. This once again testifies to the single crystallinity of the grown epitaxial layers in terms of the orientation of the GaAs(111) substrate.

Sb also plays an electrical compensating role for emerging point defects and traps, creating a deep level inside the band gap. Therefore, the concentration of the main carriers decreases, respectively, the resistivity increases, and the mobility also increases [5, 6]. This contributes to the production of a relatively medium and high-resistance crystal (as a promising material for optoelectronic devices) avoiding a heavily doped low-resistance solid solution (Table 2).

Core AFM was used to study the surface morphology of grown $(GaAs)_{1-x}(ZnSe)_x$ <Sb> films. AFM measurements of the film surface were carried out in the statistical (contact) mode. In this mode, the probe is in constant contact with the surface while the probe raster scans the sample. Figure 5 shows the surface roughness of the epitaxial layers, which is 1.28 nm high and 1.9 nm deep (the root mean square roughness (RMS) of their surface is 1.755 nm). These are rather smooth grown films [16]. The surface of the epitaxial layers is without noticeable faceting; therefore, it can be considered as a single-crystal film with a high-quality surface, grown from a saturated solution-melt (which shows the perfection of the substrate-film heterointerface (Fig. 4)). Crystals grown from a supersaturated melt solution have more pronounced and more frequent surface irregularities. The roughness of the substrate-film heterointerface indicates that the obtained films were grown from a melt solution that was not

Table 2. Some electrophysical parameters of the solid solution (GaAs)1-x(ZnSe)x before and after alloying with <Sb> at a temperature of 300 K

Sample	Conductivity type	Resistivity ρ, Ω·cm	Charge carrier concentration p, cm^{-3}	Mobility of charge carriers μp, cm^2/V·s
$(GaAs)_{1-x}(ZnSe)_x$	p	0.05÷1	$10^{18}\div2\cdot10^{19}$	30÷60
$(GaAs)_{1-x}(ZnSe)_x$ <Sb>	p	500÷1100	$3\cdot10^{16}\div10^{17}$	70÷100

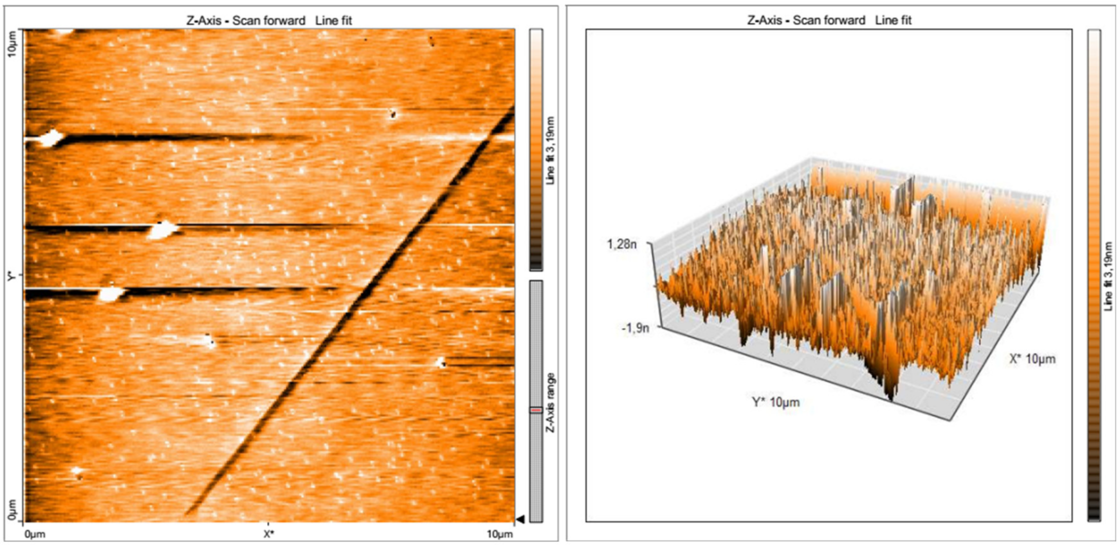

Fig. 5. 2D (a) and 3D (b) AFM images of a $(GaAs)_{1-x}(ZnSe)_x$ <Sb> film grown on a GaAs substrate.

saturated; as a result, the substrate partially dissolves [17].

4. Conclusion

This work shows the preparation of epitaxial layers of a solid solution $(GaAs)_{1-x}(ZnSe)_x$ from a limited tin solution-melt on a GaAs(100), GaAs(111) substrate at a crystallization onset temperature T_{OC} = 750°C, with forced cooling of 1 deg/min. The chemical composition and crystal structure of the grown epitaxial layers have been studied. The conditions for the optimal technological growth of the $(GaAs)_{1-x}(ZnSe)_x$ film and GaAs–$(GaAs)_{1-x}(ZnSe)_x$ structures based on them have been established. In the process of growing epitaxial layers of the $(GaAs)_{1-x}(ZnSe)$ solid solution, they were doped with antimony and it was possible to obtain crystalline films with the lowest dislocation density ($N_d = 7{\cdot}10^3$ cm^{-2}). And also antimony as a compensating impurity reduces the concentration of the main carriers (respectively, the specific resistance increases) and their mobility slightly increases. Thus, in the future, these solid solutions, as a direct-gap semiconductor material with controlled electrophysical and photoelectric properties, can be used in the field of optoelectronics.

Acknowledgements. We would like to acknowledge prof. A.V.Dolbin from B. Verkin Institute for Low Temperature Physics and Engineering for valuable advice and Associate prof. S.I.Petrushenko from V.N.Karazin Kharkiv National University for assistance in SEM-studies.

References

1. A.S.Saidov, E.A.Koshchanov, U.Nasyrov, K.Gaimnazarov, *Solar Engineering*, **6**, 23 (1998).
2. A.S.Saidov, A.Sh.Razzokov, K.Gaimnazarov, *Letters ZhTF*, **27**, 86 (2001).
3. S.Guha, H.Munekata, F.K.LeGoues, L.L.Chang, *Appl. Phys. Lett.*, **60**, 3220 (1992).
4. G.M.Blom, J.M.Woodall, *J. Mater. Electr.*, **17**, 391 (1998).
5. W.C.Mitchel, P.W.Yu, *J. Appl. Phys.*, **62**, 4781 (1987).
6. K.D.Jamison, H.C.Chen, A.Bensaoula et al., *J. Vacuum Scie, Technol.*, **A7**, 606 (1989).
7. K.Mallik, S.Dhar, S.Sinha, *Semicond. Sci. Technol.*, **9**, 1649 (1994).
8. L.Li et., *Nano Lett.*, **17**, 622 (2017).
9. M.Takemura, H.Goto, T.Ido, Japan, *J. Appl. Phys.*, **36**, 540 ?????? DOI10.1143/JJAP.36.L540
10. J.J.Davies, D.Wolverson, G.N.Aliev et al., *Scie. Technol.*, **18**, 978 (2003).
11. A.Gangopadhyay et al., *Scripta Materialia*, **225**, 115150 (2023).
12. R.Rashid, A.Mahmood, U.Aziz et al., *Opt. Mater.*, **51**, 115 (2016).
13. A.Sh.Razzokov, A.S.Saidov, S.I.Petrushenko, S.V.Dukarev, *Functional Materials*, **29**, 202, (2022).
14. A.S.Saidov, A.Sh.Razzokov, S.I.Petrushenko, S.V.Dukarov, Acta Physica Polonica A N2, **142**, 280 (2022).
15. V.M.Andreev, L.M.Dolginov, D.N.Tretyakov, Liquid Epitaxy in Technology Semiconductor Devices, Mod. Radio, Moscow (1975) [in Russian].
16. J.Yu, Y.Namba, *Appl. Phys.*, **73**, 3607 (1998).
17. C.S.Galbraith, A.E.Flood, S.Rugmai, P.Chirawatkul, *Chem. Eng. Technol.*, **39**, 199 (2016).